Biomedical Optics EXPRESS

Preliminary fsLIBS study on bone tumors

Ruby K. Gill,[1,2,6] Zachary J. Smith,[1,3,6] Ripul R. Panchal,[4] John W. Bishop,[5] Regina Gandour-Edwards,[5] and Sebastian Wachsmann-Hogiu[1,5,6,*]

[1]*Center for Biophotonics, University of California, Davis, 95616, USA*
[2]*Department of Biomedical Engineering, University of California, Davis, 95616, USA*
[3]*Department of Precision Machinery and Precision Instrumentation, University of Science and Technology of China, Hefei, Anhui, China*
[4]*Department of Neurological Surgery, University of California, Davis, 95616, USA*
[5]*Department of Pathology and Laboratory Medicine, University of California, Davis, 95616, USA*
[6]*These authors contributed equally to this work*
[*]*swachsmann@ucdavis.edu*

Abstract: The aim of this study is to evaluate the capability of femtosecond Laser Induced Breakdown Spectroscopy (fsLIBS) to discriminate between normal and cancerous bone, with implications to femtosecond laser surgery procedures. The main advantage of using femtosecond lasers for surgery is that the same laser that is being used to ablate can also be used for a feedback system to prevent ablation of certain tissues. For bone tumor removal, this technique has the potential to reduce the number of repeat surgeries that currently must be performed due to incomplete removal of the tumor mass. In this paper, we performed fsLIBS on primary bone tumor, secondary tumor in bone, and normal bone. These tissues were excised from consenting patients and processed through the UC Davis Cancer Center Biorepository. For comparison, each tumor sample had a matched normal bone sample. fsLIBS was performed to characterize the spectral signatures of each tissue type. A minimum of 20 spectra were acquired for each sample. We did not detect significant differences between the fsLIBS spectra of secondary bone tumors and their matched normal bone samples, likely due to the heterogeneous nature of secondary bone tumors, with normal and cancerous tissue intermingling. However, we did observe an increase in the fsLIBS magnesium peak intensity relative to the calcium peak intensity for the primary bone tumor samples compared to the normal bone samples. These results show the potential of using femtosecond lasers for both ablation and a real-time feedback control system for treatment of primary bone tumors.

©2015 Optical Society of America

OCIS codes: (300.0300) Spectroscopy; (300.6365) Spectroscopy, laser induced breakdown; (170.6510) Spectroscopy, tissue diagnostics; (170.4730) Optical pathology; (170.1020) Ablation of tissue.

References and links

1. A. Kumar, F. Y. Yueh, J. P. Singh, and S. Burgess, "Characterization of malignant tissue cells by laser-induced breakdown spectroscopy," Appl. Opt. **43**(28), 5399–5403 (2004).
2. A. El-Hussein, A. K. Kassem, H. Ismail, and M. A. Harith, "Exploiting LIBS as a spectrochemical analytical technique in diagnosis of some types of human malignancies," Talanta **82**(2), 495–501 (2010).
3. R. K. Gill, F. Knorr, Z. J. Smith, M. Kahraman, D. Madsen, D. S. Larsen, and S. Wachsmann-Hogiu, "Characterization of Femtosecond Laser-Induced Breakdown Spectroscopy (fsLIBS) and Applications for Biological Samples," Appl. Spectrosc. **68**(9), 949–954 (2014).
4. F. J. Fortes, J. Moros, P. Lucena, L. M. Cabalin, and J. J. Laserna, "Laser-induced breakdown spectroscopy," Anal. Chem. **85**(2), 640–669 (2012).
5. E. L. Gurevich and R. Hergenröder, "Femtosecond laser-induced breakdown spectroscopy: Physics, applications, and perspectives," Appl. Spectrosc. **61**(10), 233–242 (2007).

#250002 Received 14 Sep 2015; revised 28 Oct 2015; accepted 10 Nov 2015; published 16 Nov 2015

6. D. W. Hahn and N. Omenetto, "Laser-Induced Breakdown Spectroscopy (LIBS), Part I: Review of Basic Diagnostics and Plasma-Particle Interactions: Still-Challenging Issues Within the Analytical Plasma Community," Appl. Spectrosc. **64**(12), 335–366 (2010).
7. D. W. Hahn and N. Omenetto, "Laser-Induced Breakdown Spectroscopy (LIBS), Part II: Review of Instrumental and Methodological Approaches to Material Analysis and Applications to Different Fields," Appl. Spectrosc. **66**(4), 347–419 (2012).
8. C. Pasquini, J. Cortez, L. M. C. Silva, and F. B. Gonzaga, "Laser induced breakdown spectroscopy," J. Braz. Chem. Soc. **18**(3), 463–512 (2007).
9. R. Noll, *Laser-Induced Breakdown Spectroscopy: Fundamentals and Applications* (Springer, 2012).
10. B. M. Kim, M. D. Feit, A. M. Rubenchik, B. M. Mammini, and L. B. Da Silva, "Optical feedback signal for ultrashort laser-pulse ablation of tissue," Appl. Surf. Sci. **127-129**, 857–862 (1998).
11. D. C. Jeong, P. S. Tsai, and D. Kleinfeld, "Prospect for feedback guided surgery with ultra-short pulsed laser light," Curr. Opin. Neurobiol. **22**(1), 24–33 (2012).
12. S. H. Chung and E. Mazur, "Surgical applications of femtosecond lasers," J. Biophotonics **2**(10), 557–572 (2009).
13. B. Schwab, D. Hagner, J. Bornemann, and R. Heermann, "The use of femtosecond technology in otosurgery," in *Femtosecond Technology for Technical and Medical Applications* (Springer, 2004), pp. 211–226.
14. Y. Liu and M. Niemz, "Ablation of femural bone with femtosecond laser pulses--a feasibility study," Lasers Med. Sci. **22**(3), 171–174 (2007).
15. D. D. Lo, M. A. Mackanos, M. T. Chung, J. S. Hyun, D. T. Montoro, M. Grova, C. Liu, J. Wang, D. Palanker, A. J. Connolly, M. T. Longaker, C. H. Contag, and D. C. Wan, "Femtosecond plasma mediated laser ablation has advantages over mechanical osteotomy of cranial bone," Lasers Surg. Med. **44**(10), 805–814 (2012).
16. J. Neev, L. B. Da Silva, M. D. Feit, M. D. Perry, A. M. Rubenchik, and B. C. Stuart, "Ultrashort pulse lasers for hard tissue ablation," IEEE J. Quantum Electron. **2**(4), 790–800 (1996).
17. E. Ward, C. DeSantis, A. Robbins, B. Kohler, and A. Jemal, "Childhood and adolescent cancer statistics, 2014," CA Cancer J. Clin. **64**(2), 83–103 (2014).
18. G. R. Mundy, "Metastasis to bone: causes, consequences and therapeutic opportunities," Nat. Rev. Cancer **2**(8), 584–593 (2002).
19. A. Longhi, C. Errani, M. De Paolis, M. Mercuri, and G. Bacci, "Primary bone osteosarcoma in the pediatric age: state of the art," Cancer Treat. Rev. **32**(6), 423–436 (2006).
20. R. E. Coleman, "Metastatic bone disease: clinical features, pathophysiology and treatment strategies," Cancer Treat. Rev. **27**(3), 165–176 (2001).
21. R. E. Coleman, "Clinical features of metastatic bone disease and risk of skeletal morbidity," Clin. Cancer Res. **12**(20), 6243s–6249s (2006).
22. D. W. Kufe, R. E. Pollock, R. R. Weichselbaum, R. C. Bast, T. S. Gansler, J. F. Holland, E. Frei, J. L. Connolly, S. J. Schnitt, and H. H. Wang, "Role of the surgical pathologist in the diagnosis and management of the cancer patient," (2003).
23. S. Castiglioni and J. A. M. Maier, "Magnesium and cancer: a dangerous liason," Magnes. Res. **24**(3), S92–S100 (2011).
24. F. I. Wolf, A. R. M. Cittadini, and J. A. M. Maier, "Magnesium and tumors: ally or foe?" Cancer Treat. Rev. **35**(4), 378–382 (2009).
25. C. Kerdudo, I. Aerts, S. Fattet, L. Chevret, H. Pacquement, F. Doz, J. Michon, M. Garabedian, and D. Orbach, "Hypercalcemia and childhood cancer: a 7-year experience," J. Pediatr. Hematol. Oncol. **27**(1), 23–27 (2005).

Introduction

The basic atomic spectroscopy technique laser induced breakdown spectroscopy (LIBS) has been successfully used to distinguish different soft tissue tumors from normal tissue. In 2004, Kumar et al used nanosecond LIBS to analyze hemangiosarcomas excised from the liver of dogs. They found differences in the concentrations of calcium, copper, and sodium relative to potassium in normal and tumor tissue [1]. In 2010, Hussein et al used nanosecond LIBS to analyze breast and colorectal tumors from human subjects. They found that the concentration of both calcium and magnesium increased in tumor tissue compared to normal tissue [2]. While these publications have shown the potential of using nanosecond LIBS as a diagnostic tool, it is important to explore the use of fsLIBS for this purpose. There are significant differences between LIBS generated with nanosecond and femtosecond lasers. Because of the long pulse duration, the nanosecond laser pulse is often absorbed by the plasma plume. This results in significant heating of the plasma plume and generation of a high bremsstrahlung background. To separate the bremsstrahlung background from the LIBS signal, expensive time gating electronics must be used. Different time delays must be experimentally tested to determine the optimal acquisition settings. This is in contrast to LIBS generated with

#250002 Received 14 Sep 2015; revised 28 Oct 2015; accepted 10 Nov 2015; published 16 Nov 2015

femtosecond lasers. Femtosecond lasers do not deposit as much heat into the sample and the generated plasma plume is characterized by lower temperatures. This results in a lower signal and a significantly lower bremsstrahlung background. For this reason, femtosecond generated LIBS is much more suitable than nanosecond generated LIBS for in vivo applications [3–10].

Femtosecond lasers have been successfully used in several preliminary studies for hard tissue removal [10–16]. Their main advantage is that, compared to conventional nanosecond lasers, ultra-short pulse lasers do not deposit as much heat in the sample and therefore do not cause adverse thermal effects such as fractures [15]. It has been demonstrated in a pre-clinical study that the use of femtosecond lasers for cutting bone results in faster healing times [15]. When combined with a real-time feedback control system such as LIBS, these outcomes can be further improved. There is a growing interest in ultra-short pulsed laser surgery combined with a feedback control mechanism for high-precision cutting of bone with minimal impact to surrounding tissues [11].

A potential application for ultra-short pulsed laser surgery combined with a real-time feedback control system is bone tumor removal. Bone tumors are characterized by unusual bone formation that can either be primary or secondary. Primary bone tumors refer to those that originate from the bone cells. Primary bone tumors are amongst the ten most common type of cancer in pediatric patients [17]. This is in contrast to secondary or metastatic tumors that originate from other cancer sites [18]. Both types of bone tumors are diagnosed with non-invasive medical imaging modalities such as CT or MRI [19, 20]. Treatments for primary bone tumor include radiation therapy that is often followed by surgery to remove the tumor mass whereas radiation therapy alone is commonly used to treat cancer that has metastasized to the bone [19–21]. A major issue encountered during these surgeries is the lag time between the surgery and when the excised tumor tissue is analyzed by a pathologist. If the pathologist determines that tumor was left behind at the periphery, a second surgery must be scheduled [22].

The aim of this study is to understand the differences in femtosecond LIBS (fsLIBS) spectra of bone tumors, both primary and secondary, as compared to normal bone. If the cancerous tissue has a different fsLIBS spectrum compared to healthy bone, a real-time feedback control can be developed for the surgeon. In this scenario a femtosecond laser would be used to perform the surgery, with the fsLIBS signal generated by the laser ablation being used to inform the surgeon what tissue is being ablated. This method would allow the surgeon to identify tumor margins in real-time, thus eliminating the delay between receiving the excised tumor sample and the time it takes a pathologist to prepare sections of the excised tissue and analyze them. While others have reported that nanosecond LIBS has the power to differentiate cancerous and normal tissues, we are the first to demonstrate that *femtosecond* LIBS has this ability as well, without the need of electronic gating that is typically needed in LIBS with longer pulses. Given that femtosecond lasers are more advantageous for laser surgery applications, this work has the potential to improve the surgical outcomes and quality of life for patients with bone tumors.

Materials and methods

Sample preparation

In our experiments, we tested primary bone tumor, metastatic bone tumor and normal bone samples. These samples were excised during surgeries from consenting patients. Private patient information was de-identified through the UC Davis Cancer Center Biorepository. One primary bone tumor (osteosarcoma) sample was obtained, due to the rarity of the disease. Three metastatic bone tumor samples were tested. The metastatic bone tumor samples are labeled by the primary cancer diagnosis, which included: prostate, breast, and adenocarcinoma cancer of unknown origin. Each of the primary and metastatic tumor samples tested was compared to a region of normal bone from the same subject.

#250002 Received 14 Sep 2015; revised 28 Oct 2015; accepted 10 Nov 2015; published 16 Nov 2015

Experimental set-up

The fsLIBS measurements were performed with a set-up consisting of the following key components: a femtosecond laser, spectrometer, CCD, and a computer (Fig. 1). An Amplitude Systemes Tangerine laser with a pulse duration of 320 fs and a center wavelength of 1030 nm was used. The laser was operated at a repetition rate of 1 kHz and a pulse energy of 50 µJ for all measurements. The sample was placed on a custom-built upright microscope where an Olympus 4x, 0.1 NA air objective was used to focus the laser beam into a focal spot of 12.6 µm. A dichroic mirror reflects the laser light onto the sample and passes the emitted plasma signal toward a 35 mm focal lens that focuses the signal into a 50 µm diameter multimode fiber. The fsLIBS signal is then coupled nto an Ocean Optics 4000 spectrometer and CCD.

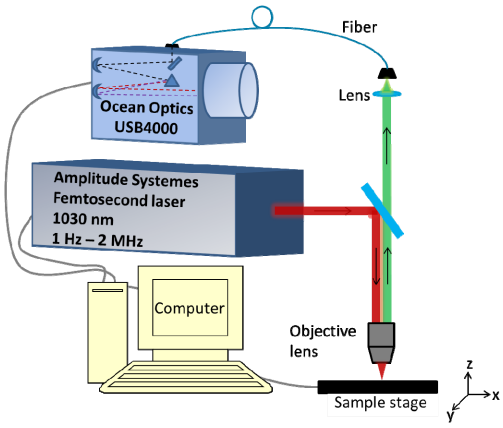

Fig. 1. Schematic diagram of the experimental set-up for the detection of the LIBS signal. The laser is focused onto the sample using an Olympus 4x, 0.1 NA microscope objective. The emitted spectra are dispersed using a spectrometer and collected with a CCD connected to a computer.

fsLIBS measurements

To perform the fsLIBS measurements, the sample was placed on the microscope stage and the laser light irradiated the sample while the stage was moved by hand. Over 20 spectra were acquired during a sample scan with a minimum acquisition time of 100 ms each. The fsLIBS spectra were analyzed with MATLAB (R2012a, The MathWorks, Natick, MA) and background subtracted using an algorithm described in Gill et al. [3]. Principal component analysis (PCA) was performed on the spectra acquired from each matching tissue set (consisting of tumor and normal tissues from the same patient).

Results

We performed laser ablation with a femtosecond laser system at a repetition rate of 1 kHz on primary bone tumor, metastatic bone tumor, and normal bone samples. First, we acquired fsLIBS spectra of the primary bone tumor and a matched normal bone sample at a repetition rate of 1 kHz to quantify changes in atomic composition (Fig. 2). The mean spectra (Fig. 2(a)) reveal an increase in the magnesium peak intensity at 516 nm and a slight decrease in the calcium peak intensity at 526 nm for the bone tumor sample compared to the normal bone sample. To further quantify the differences between the spectra, a principal components analysis (PCA) was performed. The first two PCA loadings (Fig. 2(b)) show the major spectral differences in the data set, the majority of which are visible by eye in Fig. 2(a). The first loading shows that as the magnesium peak intensity increases, the calcium peak intensity decreases. The second loading reveals changes in the calcium and sodium content of the bone. Plotting the first two scores from the PCA analysis for each spectrum from the primary bone

#250002 Received 14 Sep 2015; revised 28 Oct 2015; accepted 10 Nov 2015; published 16 Nov 2015
(C) 2015 OSA

tumor and matched normal bone shows that the majority of the acquired spectra are very well separated, as shown in Fig. 2(c). To assess the degree of separation, we performed a hierarchical clustering analysis using the first two principal component scores, as shown in the dendrogram in Fig. 3(d). The dendrogram reveals two well-separated clusters. In Fig. 2(c), each spectrum is given either a circle or triangle symbol depending on whether it was classified in cluster 1 or 2, respectively. There were very few normal spectra (2/106) that were classified as tumor whereas there are many tumor spectra (127/200) that were classified as normal bone. This overlap may be due to the presence of normal cells in the tumor region that was tested. This mixing between normal and cancerous cells can be seen in a photographic image of the bone sample shown in Fig. 3. The tumor region has a more spongy appearance compared to the normal bone region, yet clearly consists of a mixture of normal and abnormal tissues.

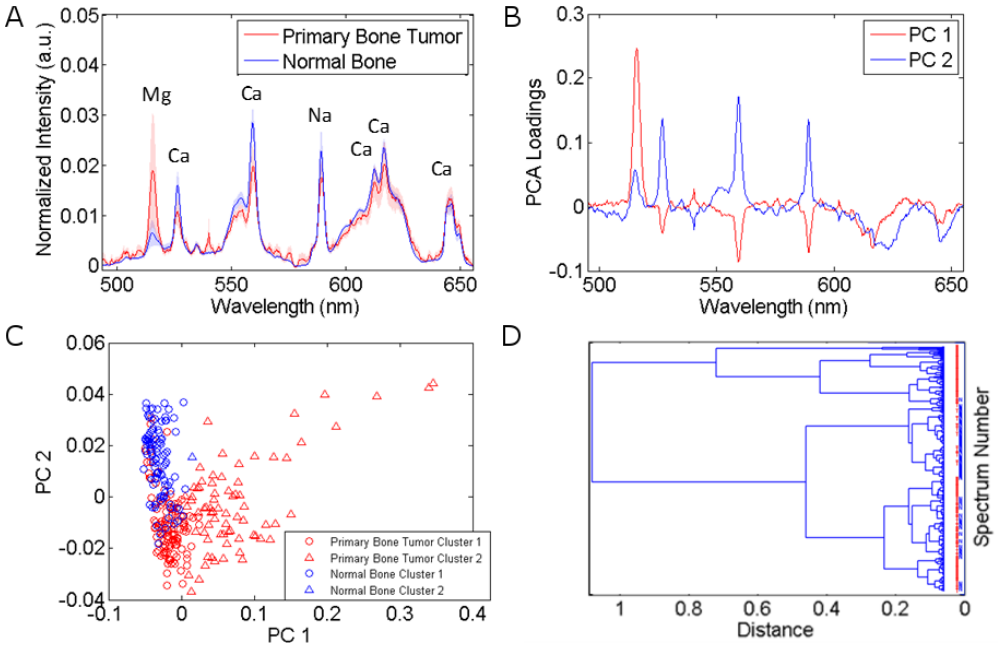

Fig. 2. fsLIBS spectra of a primary bone tumor and matched normal bone sample (A) and PCA loadings (B), PCA analysis (C), and hierarchical clustering of the all the data, where red indicated tumor and blue indicates normal bone (D).

Next, we acquired fsLIBS spectra of metastatic bone tumor and matched normal bone samples that were removed from the patient during the same surgical procedure (Fig. 4). The metastatic bone tumor samples are labeled by the primary cancer diagnosis that included: prostate cancer, breast cancer, and adenocarcinoma of unknown origin. In contrast to the results on primary tumor shown above, the averaged fsLIBS spectra for all three metastatic bone tumor samples did not show a significant difference. A subsequent PCA analysis on each of the data sets shown in the left column of Fig. 4 also showed significant overlap between the normal bone and tumor bone samples (as seen in the right column of Fig. 4). The first loading for the PCA analysis was similar to that of the primary bone tumor for each of the data sets, showing the same change in magnesium versus calcium content within the bone. However, the fsLIBS spectra of the metastatic bone and normal bone samples from the subjects with primary prostate and adenocarcinoma cancer showed large standard deviation at the magnesium peak intensity (516 nm) indicating that the spectra from both normal and metastatic bone samples were from regions with widely varying atomic composition. These results were further validated by the pathology images for the metastatic breast tumor in bone

#250002 Received 14 Sep 2015; revised 28 Oct 2015; accepted 10 Nov 2015; published 16 Nov 2015

and normal bone (Fig. 5). The pathology images show that both the nominally normal bone and metastatic bone samples contained mixtures of normal and tumor cells. Thus, the lack of separation between the two samples is to be expected. However, the inability of the surgeon to correctly determine which pieces of excised tissue were truly "normal" versus "cancerous" highlights the need for additional feedback.

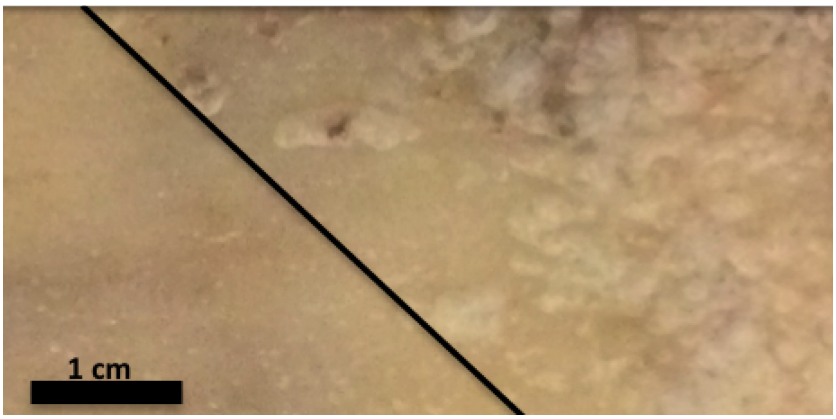

Fig. 3. Image of the tested bone sample from the subject with osteosarcoma showing the regions where the normal and tumor bone fsLIBS spectra were acquired.

We expect some natural variability between in the LIBS spectra even from normal patients. To explore this, we took the data shown in Fig. 3 from normal and cancerous bone of a primary bone tumor patient, and combined it with the data from the "normal" tissue shown in Fig. 4. We performed a PCA decomposition of this merged data set to compare the separation of tumor and normal tissue with several different "normal" bone samples. The results are shown in Fig. 6. In Fig. 6(a) we compare the PC loadings from Fig. 3(b) to those calculated from the merged data set. As is evident, the PCs of the two data sets largely overlap, confirming that the chemical differences between normal and diseased tissue is consistent even when new normal bone tissue are added to the data. Figure 6(b) shows the scores for these new PCs for the normal and cancerous tissues from the primary osteosarcoma patient, as well as the normal tissue from the secondary bone tumor patients (shown in magenta). While there is some subject-to-subject variation in the normal tissue, the overlap between the tumor and normal tissue is similar to that shown in Fig. 3(c). A cluster analysis reveals only a small number of normal spectra being classified as cancerous (21/547), while the number of cancerous spectra classified as normal is unchanged from the smaller data set (127/200).

#250002 Received 14 Sep 2015; revised 28 Oct 2015; accepted 10 Nov 2015; published 16 Nov 2015
(C) 2015 OSA

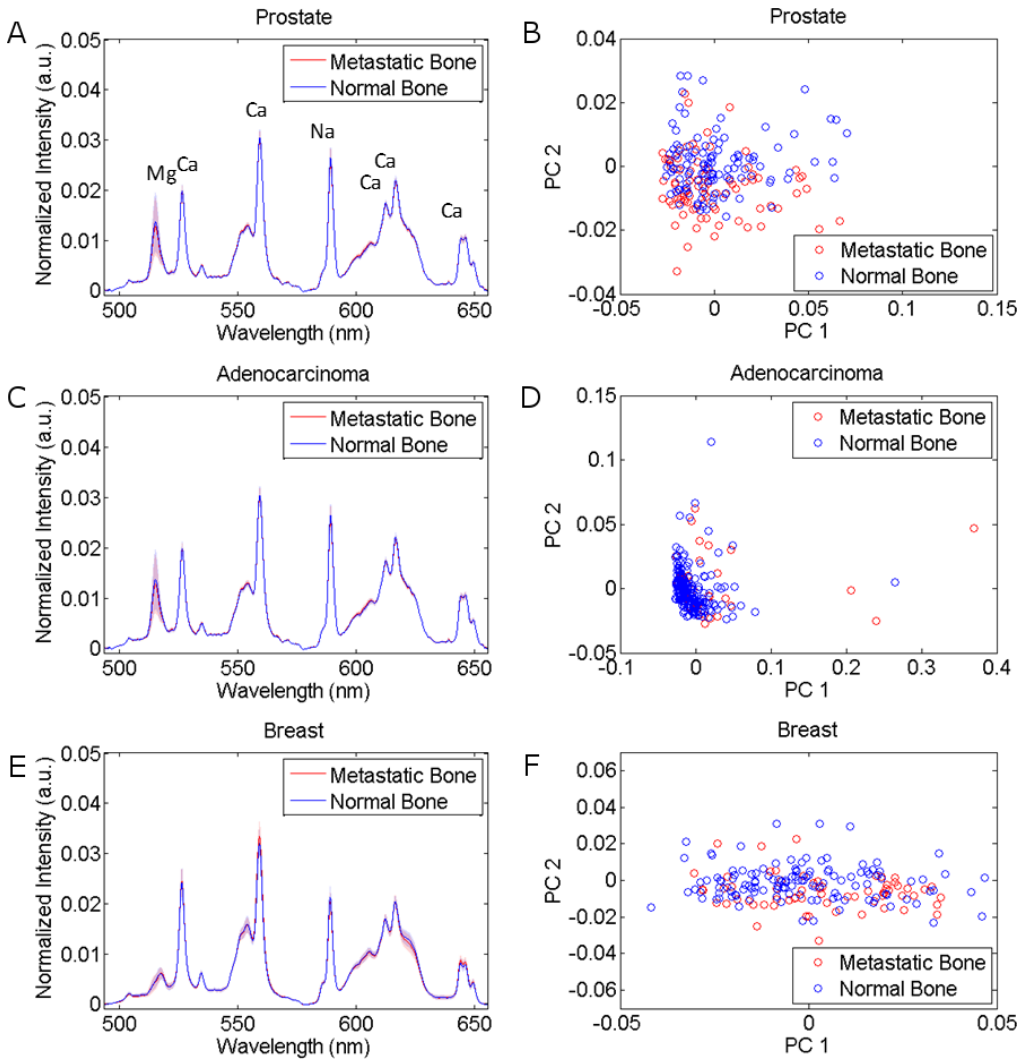

Fig. 4. fsLIBS spectra of metastatic bone tumor and matched normal bone samples (A, C, E) and PCA analysis of all the data (B, D, F).

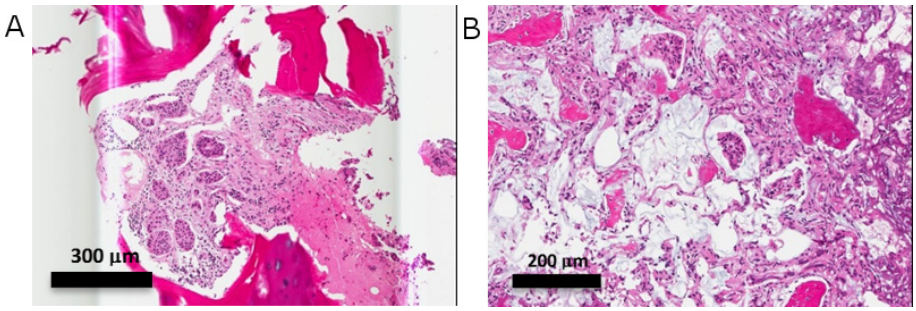

Fig. 5. Microscope images from stained pathology sections from "normal" bone (A) and metastatic breast cancer in bone (B).

#250002 Received 14 Sep 2015; revised 28 Oct 2015; accepted 10 Nov 2015; published 16 Nov 2015

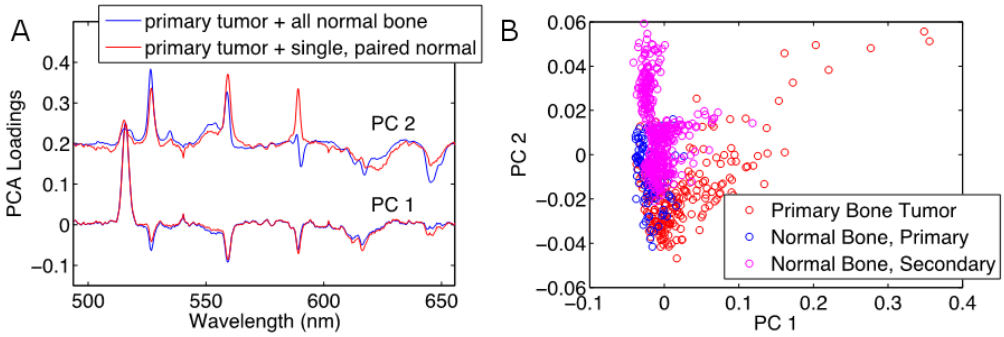

Fig. 6. PCA analysis of primary bone tumor, a paired normal bone sample, and normal bone from 3 patients with secondary bone tumors, shown in Fig. 4. (A) Comparison between PC loadings shown in Fig. 2(B) and loadings including all 4 normal bone samples. (B) PC scores for the loadings calculated from the data set including the primary bone tumor and all for normal bone samples.

Discussion

We detected significant changes in the fsLIBS signal between primary bone tumor and normal bone samples. The magnesium peak intensity (516 nm) increases relative to the calcium peak intensity (526 nm) in tumor tissue. Magnesium plays an important role in regulating cell division [23]. Although a low magnesium diet is generally thought to be a risk factor for cancer, in fact neoplastic cells preferentially uptake high concentrations of magnesium even in an overall low magnesium environment [24]. This increase magnesium concentration facilitates immortalization of the neoplastic cells. Additionally, this increase in magnesium peak intensity is consistent with the study performed by Hussein et al. on soft tissue tumors using nsLIBS, which they also attributed to magnesium having a critical role in uncontrolled tumor cell division [2]. We also observed a different dependence for the calcium peak intensity compared to the results shown by Hussein et al. We detected a decrease in calcium peak intensity in the primary bone tumor as compared to normal bone. This decrease in calcium peak intensity may be related to hypercalcemia in the blood which can occur in patients with primary bone tumors due to the increased activity of osteoclast cells that aid in the breakdown of bone [25]. This preliminary study shows the potential for fsLIBS to be used as a real-time feedback control system to ensure complete removal of a primary bone tumor thereby reducing the need for repeat surgeries. However, the overlap between fsLIBS spectra from secondary tumor and normal tissue from the same patient indicates that further work is necessary to find the optimum experimental method to reliably distinguish between healthy and diseased tissues. For example, we did not observe a significant difference in the fsLIBS spectra of metastatic tumors in bone and matched normal bone samples for the spectral region we analyzed (500-650 nm). The metastatic tumor and matched normal bone samples analyzed by a pathologist showed that there were traces of tumor tissue in both samples, and that the both metastatic and "normal" tissues were complex mixtures of cancerous and normal cells. Thus, a single fsLIBS measurement may include signal from both cancerous and normal cells, no matter whether one is measuring metastatic or "normal" tissue from a diseased patient. Thus, a system that acquires a series of LIBS spectra to map out the spatial distribution of signals may be necessary for surgical guidance. One possible explanation why we did not observe a change in the fsLIBS spectra between metastatic bone tumor and normal bone may be because the primary cancer cells diffuse throughout the body and may not cause a metabolic change in other cell types (such as bone). As seen in Fig. 5, metastatic tumors are mixed on a microscopic level with healthy tissue, presenting a challenge for surgical resection as both metastatic and normal bones. Our sampling method involves averaging signals from throughout the entire resected sample, potentially causing us to primarily sample normal bone. Therefore, a more refined sampling strategy that takes into account the microscopic

#250002 Received 14 Sep 2015; revised 28 Oct 2015; accepted 10 Nov 2015; published 16 Nov 2015

variability of metastatic bone tumors may observe more significant differences between normal and metastatic bone tissue. However, because metastatic bone tumors are indicative of a very late stage form of cancer that has spread throughout the body, it may not be useful to use femtosecond laser ablation in combination with fsLIBS to ensure complete removal of tumor cells when other treatments (or palliative care) that can treat the cancer systemically are typically used instead of surgery in these cases. However, our study shows for the first time that femtosecond lasers, which are preferred for ultrashort-pulsed laser surgeries due to better cutting and lower thermal damage, can be used to generate fsLIBS spectra that distinguish between tumorous and normal tissues. These preliminary results suggest future work, such as generating spatial maps of LIBS signals or exploring other areas of the LIBS spectrum at blue and UV wavelengths, that will improve the diagnostic potential of fsLIBS for surgical applications.

Acknowledgments

Specimens were provided by the UC Davis Comprehensive Cancer Center Biorepository, which is funded by the National Cancer Institute. Funding for this research was provided by the NSF Program Accelerating Innovation Research: Creation of an Ecosystem for Biophotonics Innovation, award number 1127888; and by UC Davis Cancer Center and LLNL Fitzpatrick Fund.